

## Pb nanoribbons on the Si(553) surface

M. Kopciuszynski, P. Dyniec, M. Krawiec, P. Łukasik, M. Jałochowski, and R. Zdyb\*

*Institute of Physics, Maria Curie-Skłodowska University, 20-031 Lublin, Poland*

(Received 10 September 2013; published 22 October 2013)

The crystallographic structure and morphology of the Si(553) surface ordered by Pb atoms are investigated with the reflection high-energy electron diffraction (RHEED), scanning tunneling microscopy (STM) and density functional theory (DFT) techniques. Adsorption of 1.3 monolayers of Pb, and a subsequent gentle annealing, causes regular distribution of Si atomic steps over the macroscopic sample area. The step periodicity is exactly the same as in the case of the Au-induced Si(553). However, the hybridization between Pb and Si atoms is weaker, as compared to Au and Si atoms on the Si(553) surface. Instead of two Au atomic chains strongly bonded to Si atoms, Pb forms a five-atom-wide nanoribbon on each Si(111) terrace. The simulated STM topography images obtained with the DFT calculations agree very well with the results obtained in the RHEED and STM experiments.

DOI: [10.1103/PhysRevB.88.155431](https://doi.org/10.1103/PhysRevB.88.155431)

PACS number(s): 61.05.jh, 61.46.Km, 68.37.Ef, 68.43.Bc

### I. INTRODUCTION

Vicinal surfaces with regular distribution of steps serve as perfect templates for self-organization of one-dimensional structures. The width of nanostructures and the distance between them can be tuned to the atomic scale. The angle at which surface is cut in respect to a low Miller index plane defines the terrace width and therefore also the separation between the nanostructures. On the other hand, a number of adsorbed foreign atoms defines the width of nanostructures ranging from single- to multiatom chains on each terrace.

Beside its technological importance, silicon, which reveals a bulk band gap around the Fermi level, allows to grow structures that are supposed to be electronically decoupled from the substrate. Therefore vicinal silicon surfaces with regular distribution of steps are widely used to seek and study new phenomena associated with one-dimensional metallic nanostructures. Among the most spectacular are the breakdown of the Fermi liquid theory, the Peierls distortion, charge density waves, and one-dimensional diffusion of atoms, to name a few.<sup>1–6</sup>

Vicinal surfaces that form perfect arrays of monatomic steps and (111) terraces of several lattice constants in width have been studied for many years and obtained for different silicon planes.<sup>7,8</sup> Well-known examples are the Si(557) surface with the coverage of 0.20 ML Au, Si(335) with 0.28 ML, and Si(553) with 0.48 ML Au. In particular, the Si(553)-Au surface consists of (111) terraces of  $4\frac{1}{3} \times a_{[11\bar{2}]} = 14.41 \text{ Å}$  in width ( $a_{[11\bar{2}]} = 3.325 \text{ Å}$  is the Si lattice constant along  $[11\bar{2}]$ ) separated by monatomic steps. The Si(553)-Au surface was studied in a great detail by number of techniques including STM, angle-resolved photoelectron spectroscopy (ARPES), x-ray diffraction, and DFT (see Refs. 8–15, and references therein).

All mentioned surfaces are ordered after deposition of a proper amount of Au and annealing at about 1000 K. The high temperature is necessary to form Si-Au eutectic alloy to rearrange the Si(111) terraces and to incorporate the Au atoms into the native Si lattice. As a result, the Au atoms are strongly bonded to the Si atoms and a desired one-dimensional character of the Au atomic chains is governed mainly by interaction with Si.

In this report we present a new system of Pb nanoribbons on ordered vicinal surface. Since Pb atoms are immiscible with Si,

the nanostructures are weakly bonded to the substrate and the Si(553) substrate atoms remain in their original bulk positions, and both should be relatively well electronically separated.

### II. METHODS

#### A. Experimental

The experiments have been performed in an ultrahigh vacuum system with the base pressure in the middle of  $10^{-11}$  mbar range. The system is equipped with the Omicron VT STM, the RHEED apparatus, Pb deposition source, and quartz crystal monitor. The *p*-type B-doped vicinal Si(553) sample with the specific resistivity of  $0.14 \text{ Ω cm}$  at room temperature (RT) was used in experiments. The sample was cleaned in the standard way by several flashes up to 1500 K. The Pb layer was grown at RT and annealed up to about 250 °C. Hereafter, the Si(553) surface covered with 1.3 ML Pb we call as Si(553)-Pb. Throughout the paper 1 ML corresponds to the density of atoms in a half of the bulk terminated Si(111) bilayer ( $7.84 \times 10^{14} \text{ atoms/cm}^2$ ). The STM and RHEED measurements were performed at 300 and 110 K, respectively.

#### B. Details of calculations

The calculations have been performed within local density approximation to density functional theory<sup>16</sup> as implemented in the SIESTA code.<sup>17–20</sup> Troullier-Martins norm-conserving pseudopotentials were used.<sup>21</sup> A double- $\zeta$  polarized (DZP) basis set was used for all the atomic species.<sup>18,19</sup> Due to a large supercell, only three nonequivalent *k* points for a Brillouin zone sampling and a real-space grid equivalent to a plane-wave cutoff 100 Ry were employed. The Si(553) slab has been modeled by four silicon double layers and a vacuum region of 17 Å. All the atomic positions, except the bottom layer, were fully relaxed until the maximum force was less than 0.04 eV/Å.

### III. RESULTS

Figure 1(a) presents the RHEED pattern of the Si(553)-Pb surface. The pattern shows a set of parallel diffraction streaks located on the 0th Laue zone. It resembles the RHEED pattern of the Si(553)-Au surface or of other vicinal surfaces

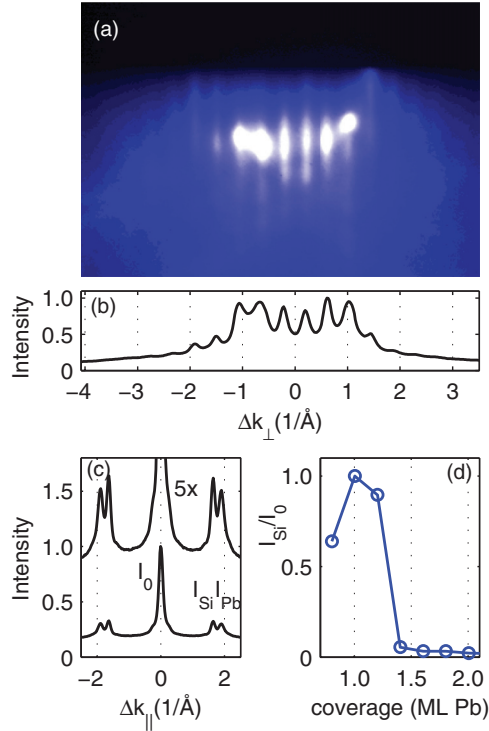


FIG. 1. (Color online) (a) RHEED pattern of Si(553)-Pb recorded with electron beam parallel to the step edges. (b) Intensity profile from the RHEED pattern of (a). (c) Intensity profile taken from the RHEED pattern with electron beam perpendicular to the step edges. (d) Ratio of the intensity of Si (10) and (00) diffraction spots vs Pb coverage.

ordered with Au atoms.<sup>7,22</sup> The streaks are perpendicular to the macroscopic plane of the Si(553) crystal surface suggesting a regular distribution of the steps. The average distance between the streaks equals  $0.42 \pm 0.01 \text{ \AA}^{-1}$ , Fig. 1(b), and corresponds to the period of  $14.95 \pm 0.40 \text{ \AA}$ . The obtained value agrees very well with the distance between the step edges of the ideal Si(553) plane ( $14.75 \text{ \AA}$ ) and implies that the surface is built of  $4\frac{1}{3} \times a_{[11\bar{2}]}$  wide (111) terraces. The RHEED pattern recorded with e-beam in the perpendicular direction (not presented here) shows a number of spots and streaks from which the intensity profile is displayed in Fig. 1(c). The peaks which are close to the Si peaks appear after deposition of the Pb layer. They are located at the scattering vector of  $1.86 \pm 0.02 \text{ \AA}^{-1}$  and indicate a periodicity of  $3.37 \pm 0.05 \text{ \AA}$  along  $[1\bar{1}0]$ . Assuming that additional periodicity is due to the distance between the Pb atoms, one can notice that eight Pb interatomic distances ( $26.96 \text{ \AA}$ ) correspond to seven Si lattice constants in this direction ( $7 \times a_{[1\bar{1}0]} = 26.88 \text{ \AA}$ ).

Figure 1(d) shows a ratio of the intensity of the Si (10) spot to the intensity of the (00) spot. A sudden drop of the Si diffraction spot intensity ratio at about  $\Theta_N = 1.3 \text{ ML Pb}$ , and its almost constant value above this critical coverage, clearly indicates that the surface is covered by Pb with a constant thickness which is independent on the amount of the predeposited Pb.

From the RHEED data, it follows that the density of Pb atoms along the  $[1\bar{1}0]$  direction is 8/7 times higher than that of Si atoms. Taking the Pb coverage as  $1.3 \text{ ML}$ , we conclude

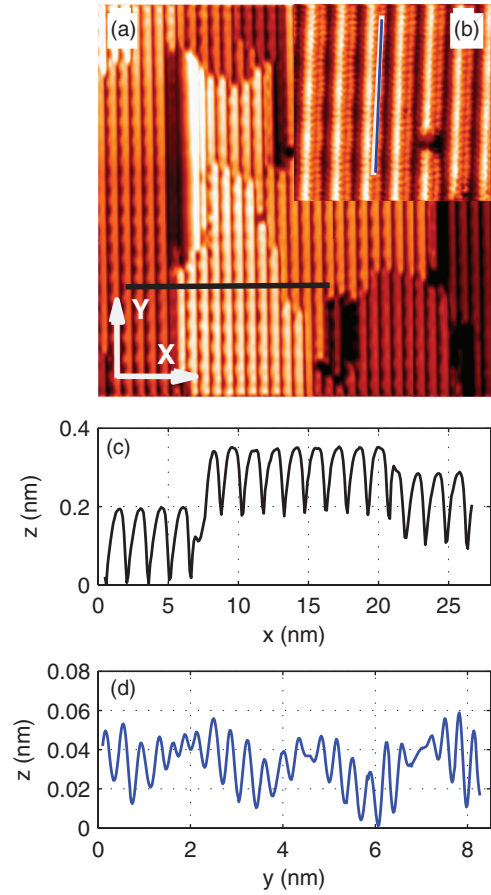


FIG. 2. (Color online) (a)  $50 \text{ nm} \times 50 \text{ nm}$  STM image of Si(553)-Pb.  $U = -0.3 \text{ V}$ ,  $I = 1 \text{ nA}$ . (b)  $8 \text{ nm} \times 8 \text{ nm}$  STM image of Si(553)-Pb,  $U = +0.3 \text{ V}$ ,  $I = 1 \text{ nA}$ . (c) Profile taken along the line shown in (a). (d) Profile taken along the line shown in (b).

that there are  $N = 5$  Pb atomic rows ( $N = 1.3 \times 4\frac{1}{3} \times 7/8 = 4.93 \simeq 5$ ) on each Si(111) terrace.

The STM measurements corroborate the conclusions of the RHEED experiments. Figure 2(a) shows a large area STM topography image of the Si(553)-Pb surface. A clear long-range order in the distribution of terraces is visible. A profile taken across the steps, the horizontal line in Fig. 2(a), indicates terraces with the width of  $14.7 \pm 0.2 \text{ \AA}$ . The obtained distance is very close to the distance between the steps of the ordered Si(553)-Au surface ( $14.75 \text{ \AA}$ ). Figure 2(a) shows several Si(553) domains that are separated by single or double steps in the  $[553]$  direction. According to the STM profile, Fig. 2(c), the single step height equals  $0.68 \pm 0.07 \text{ \AA}$ , in agreement with the value based on the silicon lattice constant ( $0.71 \text{ \AA}$ ). Moreover, the STM image shows clear periodic features along the step edges. The average periodicity of  $26.6 \pm 1.0 \text{ \AA}$  agrees very well with the seven silicon lattice constants along  $[1\bar{1}0]$  ( $26.88 \text{ \AA}$ ). The same periodic features are visible in the STM image recorded with the positive polarization, Fig. 2(b). This high resolution image presents rows of atom-like features with different intensities. Moreover, the round features in each row differ from each other revealing different intensities. It is also important to notice that the distance between the observed bright features changes. The profile taken along the line drawn in the STM

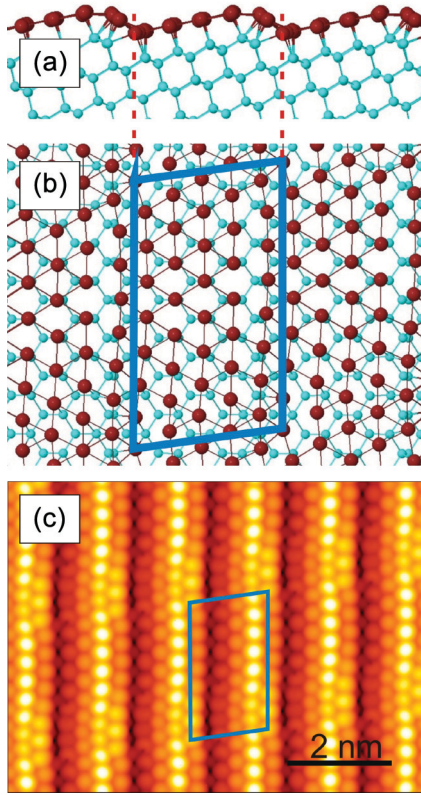


FIG. 3. (Color online) Structural model (a) and (b), and simulated STM image (c) of Si(553)-Pb. Topmost atoms in (a) denote Pb.

image indicates distances between 2.64 and 3.91 Å, Fig. 2(d). The average distance of 3.35 Å is in a perfect agreement with the interatomic distance obtained in the RHEED experiments (3.37 Å).

The above experimental findings (i) the regular distribution of steps with the terrace width of  $4\frac{1}{3} \times a_{[112]}$ , (ii) the average Pb lattice constant of 3.37 Å along  $[1\bar{1}0]$ , and (iii) the optimal coverage of about 1.3 ML implying five Pb atom rows on each (111) terrace, have been used as the input parameters to model the surface by the DFT calculations. The results of the calculations are shown in Fig. 3. The obtained structural model of the Si(553)-Pb surface reflects the assumptions and reveals additional features in the crystallographic structure of the Pb overlayer. The Pb atoms do not lay along the straight lines parallel to  $[1\bar{1}0]$ . They are periodically, with the period of seven Si lattice constants, displaced in the perpendicular direction. Three rows of atoms located in the middle of the terrace have a relatively small displacement from  $[1\bar{1}0]$ ; those located at both sides of the step edge reveal the largest deviations from the straight line. The calculations indicate that the atoms sitting at the edge of the neighboring terraces have lower number of bonds with the surrounding atoms, compared to the atoms located in the middle of terrace. The resulting curved chains of Pb atoms agree with the STM data, Fig. 2. The observed displacement of atoms from the straight line is responsible for observed different distances between the bright features in the STM images. According to the calculations they range between 2.84 Å and 3.68 Å with the average of 3.34 Å.

The STM image simulated within the Tersoff-Hamann approach<sup>23</sup> is presented in Fig. 3(c). It shows a constant

current mode image of  $6 \times 8 \text{ nm}^2$  of Si(553)-Pb for the sample bias  $U = +0.3 \text{ V}$ . The STM intensity variation between the rows of atoms and its modulation along the rows are the characteristic features of the image similar as observed in the STM experiment (see Fig. 2).

#### IV. DISCUSSION

Among well-known superstructures as, e.g.,  $(\sqrt{3} \times \sqrt{3})$  or  $(\sqrt{7} \times \sqrt{3})$  the phase diagram of Pb on a flat Si(111) surface reveals a number of ordered phases which are known as “devil’s staircase.”<sup>24</sup> Our study does not reveal any of the previously observed phases. The obtained structure can be explained by the existence of five Pb chains laying on top of Si atoms with the assumption of 8/7 times denser packing of Pb atoms along  $[1\bar{1}0]$ . The discussed model indicates that there is no intermixing between Pb and Si atoms and the Pb adlayer should be rather considered as similar to the Pb monolayer grown on a flat Si(111) surface. Indeed, the arrangement of the Pb atoms is in part similar to a model of Pb monolayer grown on flat Si(111) surface with the  $(7 \times 7)$  reconstruction.<sup>25</sup> According to the authors of Ref. 25 the Pb layer is strongly compressed resulting in the decrease of the nearest neighbor distance from 3.50 Å in the bulk Pb to 3.35 Å. Similar, a smaller lattice constant of 3.35 Å has also been observed in Pb layers grown on the vicinal Si(335) surface,<sup>26</sup> which is in perfect agreement with the value determined in the present experiment.

It is important to notice that the bare vicinal surface annealed at about 250 °C does not lead to the same ordering as with the Pb adlayer. According to Ref. 27 the bare Si(553) surface consists of (331) facets and (111) terraces with  $(7 \times 7)$  and  $(5 \times 5)$  superstructures. Thus the questions appear why does silicon surface undergo a transition to the ordered state under the influence of Pb atoms at such low temperatures and why does it happen for the Pb coverage exceeding 1 ML?

To answer the first question, we notice that the samples were firmly clamped by two clips and the annealing produces temperature gradient along the sample. Upon annealing the surface rearranges, leaving the hottest center of the sample covered with the well-ordered Pb atomic chains. The STM images taken away from the sample center reveal the presence of Pb thicker than 1 ML. Thus, during the annealing, excess of Pb is swept from the sample center and accumulated in colder regions of the sample.

The bare vicinal (553) silicon surface consists of many dangling bonds. In order to reduce the energy cost, the number of dangling bonds is reduced by formation of superstructures, like  $(7 \times 7)$ , if enough wide (111) terraces exist, or dimers, or higher order multimers. The DFT calculation and experiments indicate that there is a dimerization of atoms at the step edges. This is opposite to the case of the Si vicinal surfaces stabilized by Au atoms where no dimerization is observed. The steps with dimers have fewer dangling bonds than nondimerized steps reducing their energy. Therefore one might naively assume that the dimerized steps are strongly favored. However, the dimerized steps contribute to a tensile stress in the direction perpendicular to the step edges. For wide terraces, this stress is elastically relieved, so that the dimerized steps are favored. For very narrow terraces, however, this mechanism is much

weaker or not available. The resulting energy penalty may be higher than the energy gain from the dangling-bond reduction. Our DFT calculations indicate that the Pb atoms are weakly bonded to the surface [1.19 eV per Pb atom, which is about two times lower than for a Au atom incorporated in the Si(553)-Au surface]. Nevertheless, they form metallic bonds between themselves and, therefore, do not form new dangling bonds at the surface. In addition, as negative charge donors, they reduce dangling bonds and at the same time do not lead to the dimerization of silicon atoms. This in turn does not lead to the appearance of stress in the direction perpendicular to the step edges and therefore avoids step bunching or faceting. Finally, this results in the uniform distribution of steps on a surface. On the other hand, at lower coverage the Pb atoms tend to build monatomic chains.<sup>28</sup> This does not prevent dimerization of atoms and therefore a higher Pb coverage is necessary to avoid the stress. Although the above scenario can be considered as a hypothesis a similar scenario based on a first principle calculations has been used to explain the periodic array of row structures observed on Si(114).<sup>29</sup>

Interestingly, similar surface ordering has been reported for the Si(557) surface.<sup>30</sup> However, in that case deposition of 1.3 ML Pb results in the appearance of the (223) facets and wide (111) terraces. The authors report the existence of five Pb chains on each (111) terrace of the (223) facet. In the case of that facet, the (111) terraces are  $4\frac{2}{3} \times a_{[11\bar{2}]} = 15.52 \text{ \AA}$  wide, which is very close to the width of (111) terraces of

the (553) plane. Keeping in mind that the residual coverage is approximately the same as in our experiments, this suggests that five Pb chains per each (111) terrace is for some reason a very stable structure. To answer the question what is behind the observed stability, still more studies have to be done. It would be interesting to check whether the (223) plane gives a long-range order of steps induced by the same amount of Pb.

## V. SUMMARY

In conclusion, we have studied the silicon vicinal Si(553) surface covered with 1.3 ML of Pb. Both employed experimental methods, RHEED and STM, indicate regular distribution of steps over a macroscopic size sample area induced by the presence of Pb atoms. The Si(553)-Pb surface reveals almost a perfect order similar to the well-known Si(553)-Au surface with the same step distance. The DFT calculations corroborate the experimental findings and give a more detailed insight on the structural character of the Pb overlayer. The Pb nanoribbons are apparently weakly coupled to the substrate, thus are promising structures for studying of, e.g., quantum size effects in metallic ultrathin films with a precisely defined width.

## ACKNOWLEDGMENTS

This work has been supported by the National Science Center under Grant No. 2011/01/B/ST3/04450.

\*zdybr@hektor.umcs.lublin.pl

<sup>1</sup>S. Tomonaga, *Prog. Theor. Phys.* **5**, 544 (1950).

<sup>2</sup>J. M. Luttinger, *J. Math. Phys.* **4**, 1154 (1963).

<sup>3</sup>R. F. Peierls, *Quantum Theory of Solids* (Clarendon, Oxford, 1955).

<sup>4</sup>P. Nita, M. Jałochowski, M. Krawiec, and A. Stępnik, *Phys. Rev. Lett.* **107**, 026101 (2011).

<sup>5</sup>M. Krawiec and M. Jałochowski, *Phys. Rev. B* **87**, 075445 (2013).

<sup>6</sup>T. Giamarchi, *Quantum Physics in One Dimension* (Oxford University Press, New York, 2004).

<sup>7</sup>M. Jałochowski, M. Stróżak, R. Zdyb, *Surf. Sci.* **375**, 203 (1997).

<sup>8</sup>J. N. Crain, J. L. McChesney, Fan Zheng, M. C. Gallagher, P. C. Snijders, M. Bissen, C. Gundelach, S. C. Erwin, and F. J. Himpsel, *Phys. Rev. B* **69**, 125401 (2004).

<sup>9</sup>I. Barke, F. Zheng, S. Bockenhauer, K. Sell, V.v. Oeynhausen, K. H. Meiwes-Broer, S. C. Erwin, and F. J. Himpsel, *Phys. Rev. B* **79**, 155301 (2009).

<sup>10</sup>J. N. Crain, A. Kirakosian, K. N. Altmann, C. Bromberger, S. C. Erwin, J. L. McChesney, J.-L. Lin, and F. J. Himpsel, *Phys. Rev. Lett.* **90**, 176805 (2003).

<sup>11</sup>J. R. Ahn, P. G. Kang, K. D. Ryang, and H. W. Yeom, *Phys. Rev. Lett.* **95**, 196402 (2005).

<sup>12</sup>S. Riikonen and D. Sanchez-Portal, *Phys. Rev. B* **77**, 165418 (2008).

<sup>13</sup>W. Voegeli, T. Takayama, T. Shirasawa, M. Abe, K. Kubo, T. Takahashi, K. Akimoto, and H. Sugiyama, *Phys. Rev. B* **82**, 075426 (2010).

<sup>14</sup>M. Krawiec, *Phys. Rev. B* **81**, 115436 (2010).

<sup>15</sup>S. C. Erwin and F. J. Himpsel, *Nat. Commun.* **1**, 58 (2010).

<sup>16</sup>J. P. Perdew and A. Zunger, *Phys. Rev. B* **23**, 5048 (1981).

<sup>17</sup>P. Ordejon, E. Artacho, and J. M. Soler, *Phys. Rev. B* **53**, R10441 (1996).

<sup>18</sup>D. Sanchez-Portal, P. Ordejon, E. Artacho, and J. M. Soler, *Int. J. Quantum Chem.* **65**, 453 (1997).

<sup>19</sup>E. Artacho, D. Sanchez-Portal, P. Ordejon, A. Garcia, and J. M. Soler, *Phys. Status Solidi B* **215**, 809 (1999).

<sup>20</sup>E. Artacho, E. Anglada, O. Dieguez, J. D. Gale, A. Garcia, J. Junquera, R. M. Martin, P. Ordejon, J. M. Pruneda, D. Sanchez-Portal, and J. M. Soler, *J. Phys.: Condens. Matter* **20**, 064208 (2008).

<sup>21</sup>N. Troullier and J. L. Martins, *Phys. Rev. B* **43**, 1993 (1991).

<sup>22</sup>R. Zdyb, M. Stróżak, M. Jałochowski, *Vacuum* **63**, 107 (2001).

<sup>23</sup>J. Tersoff and D. R. Hamann, *Phys. Rev. Lett.* **50**, 1998 (1983); *Phys. Rev. B* **31**, 805 (1985).

<sup>24</sup>M. Hupalo, J. Schmalian, and M. C. Tringides, *Phys. Rev. Lett.* **90**, 216106 (2003).

<sup>25</sup>H. H. Weitering, D. R. Heslinga, and T. Hibma, *Phys. Rev. B* **45**, 5991 (1992).

<sup>26</sup>R. Zdyb, *Appl. Surf. Sci.* **254**, 4408 (2008).

<sup>27</sup>S. Hara, M. Yoshimura, and K. Ueda, *Jpn. J. Appl. Phys.* **47**, 6102 (2008).

<sup>28</sup>P. Nita, G. Zawadzki, M. Krawiec, M. Jałochowski, *Phys. Rev. B* **84**, 085453 (2011).

<sup>29</sup>S. C. Erwin, A. A. Baski, and L. J. Whitman, *Phys. Rev. Lett.* **77**, 687 (1996).

<sup>30</sup>M. Czubanowski, A. Schuster, S. Akbari, H. Pfnür, and C. Tegenkamp, *New J. Phys.* **9**, 338 (2007).